Mon. Not. R. Astron. Soc. **000**, 1—10 (????) Printed 1 February 2008 (MN LATEX style file v1.4)

The phase function for stellar acoustic oscillations - IV. Solar-like stars

F. Pérez Hernández[1⋆] and J. Christensen-Dalsgaard [2†]

[1] *Instituto de Astrofísica de Canarias, E-38200 La Laguna, Tenerife, Spain*
[2] *Teoretisk Astrofysik Center, Danmarks Grundforskningsfond and Institut for Fysik og Astronomi, Aarhus Universitet, DK-8000 Aarhus C, Denmark*

Accepted ????. Received ????; In original form 1997 June ??

ABSTRACT

In recent years there has been some progress towards detecting solar-like oscillations in stars. The goal of this challenging project is to analyse frequency spectra similar to that observed for the Sun in integrated light. In this context it is important to investigate what can be learned about the structure and evolution of the stars from such future observations. Here we concentrate on the structure of the upper layers, as reflected in the phase function. We show that it is possible to obtain this function from low-degree p modes, at least for stars on the main sequence. We analyse its dependence on several uncertainties in the structure of the uppermost layers. We also investigate a filtered phase function, which has properties that depend on the layers around the second helium ionization zone.

Key words: sun: interior – sun: oscillations – stars: oscillations

1 INTRODUCTION

Since the successful development of helioseismology in the last few decades, the interest in extending the work to other stars has become clear. However, the small amplitudes expected in the power spectra of stars with solar-like oscillations makes this a very difficult task and to date no unambiguous detection has been made. The main limitation is the atmospheric noise.

On the other hand, these stellar spectra are expected to have regular patterns that can be detected even without a full determination of the p-mode frequencies. Some efforts have been made in this direction (Brown et al. 1991; Pottasch, Butcher & van Hoesel 1992; Kjeldsen et al. 1995). The most interesting parameters that can be obtained in this limit are the so-called small and large separations, as demonstrated by several theoretical analyses (e.g. Christensen-Dalsgaard 1984, 1988, 1993; Ulrich 1986; Gough 1987; Gough & Novotny 1993).

However, the full power of asteroseismology for solar-like stars would, as in the case of helioseismology, require extensive determination of individual p-mode frequencies. In fact, once the observed amplitudes are above the noise level, a few weeks of observations will be enough to obtain accurate frequency measurements. In the near future there will be space missions devoted to asteroseismology (Baglin 1991; Catala et al. 1995) which, we hope, will give the first firm results on this issue. With these future observations in mind, in this paper we shall assume that a full set of low-degree ($l \leq 2$) p-mode frequencies are available in a given frequency range. We do not consider modes of higher degree because they cannot be detected with simple photometric observations. Also, we suppose that the radial order n and the degree l of the modes are known, and, of course, that the frequencies have been corrected for their rotational splittings. The determination of n and l requires comparison with the models but for solar-like stars on the main sequence, such as we shall consider here, it is plausible to assume that this is possible without any uncertainty.

As in the solar case, a direct comparison of theoretical and observed frequencies would be inconclusive. However, stellar acoustic oscillations satisfy a simple asymptotic relation which allows the separation of the contribution of the upper layers, such as the convective envelope, from that of the deep interior. This relation has been used extensively in the solar case, for instance to obtain the sound speed (e.g. Christensen-Dalsgaard, Gough & Thompson 1989) and to analyse the upper layers (e.g. Pérez Hernández & Christensen-Dalsgaard 1994b). Since for the distant stars we expect to detect only low-degree modes, we re-analyse the relation in this context. A similar investigation was carried out recently by Lopes et al. (1997), to investigate what would be the diagnostic potential of observing solar-like oscillations in the star β Virginis.

Analysis of observations of low-degree solar p-modes is

⋆ E-mail: fph@iac.es
† E-mail: jcd@obs.aau.dk

illustrative of what can be inferred for other stars. Thus we first present an analysis of the observations by Lazrek et al. (1997), obtained with the GOLF instrument on the SOHO spacecraft. Having demonstrated that it is possible to carry out the asymptotic analysis for stars, we concentrate our work on the upper layers as probed by the so-called phase function. We investigate the information that can be obtained from this function, taking into account the plausible accuracy of the frequency determinations. We pay particular attention to the second helium ionization zone.

2 THE SUN AS A STAR

2.1 The phase function for low-degree modes

Neglecting the perturbations in the gravitational potential and considering the waves locally as plano-parallel under constant gravity, the frequencies of p modes satisfy the asymptotic relation (Deubner & Gough 1984)

$$\frac{\pi(n+\epsilon)}{\omega_{nl}} \simeq \int_{r_1}^{r_2} \left[1 - \frac{\omega_{\rm c}^2}{\omega^2} - \frac{S_l^2}{\omega^2}\left(1 - \frac{N^2}{\omega^2}\right)\right]^{1/2} \frac{{\rm d}r}{c} \,. \qquad (1)$$

Here ω is the angular frequency, c the adiabatic sound speed, N the buoyancy frequency, $\omega_{\rm c}$ the cut-off frequency and S_l the Lamb acoustic frequency. The integral is over radius r with the limits r_1 and r_2 defined by the vanishing of the bracket in the integral. In principle, the asymptotic theory gives $\epsilon = -1/2$ but since close to the surface the asymptotic conditions are not satisfied, ϵ is assumed to be a function of frequency, yet to be determined – for low-degree modes its dependence on l is negligible.

It is interesting to note that with the sole assumption that the perturbations in the gravitational potential can be neglected, equation (1) still holds in the asymptotic limit, provided $\omega_{\rm c}$ and N are replaced by more general functions (Gough 1996).

For the Sun, and many other stars, equation (1) can be further approximated to yield a very useful relation. If there is a point r_0 – usually in the convective envelope – such that $|N^2(r)| \ll \omega^2$ and $\omega_{\rm c}^2(r) \ll \omega^2$ for $r < r_0$ and $S_l^2 \ll \omega^2$ for $r > r_0$, then it can be shown that equation (1) can be approximated by (e.g. Christensen-Dalsgaard & Pérez Hernández 1992)

$$\frac{\pi n}{\omega_{nl}} \simeq F(\omega/L) - G(\omega) \,, \qquad (2)$$

where

$$F(w) = \int_{r_{\rm t}}^{R} \left(1 - \frac{c^2}{w^2 r^2}\right)^{1/2} \frac{{\rm d}r}{c} \qquad (3)$$

and

$$G(\omega) = \frac{\pi\alpha(\omega)}{\omega} \,. \qquad (4)$$

Here $L = l + 1/2$, l being the degree of the mode, and $w = \omega/L$. The integral in equation (3) is from the lower turning point $r_{\rm t}$ (defined by the vanishing of the bracket in the integral) to the surface radius R. Finally, the phase function $\alpha(\omega)$ depends on conditions near the stellar surface.

This phase function can be computed from the structure of the upper layers of a stellar model, by fitting numerically computed eigenfunctions to an asymptotic approximation at a point where the latter is valid (see Christensen-Dalsgaard & Pérez Hernández 1992). We denote the phase function obtained in this way $\alpha_{\rm as}(\omega)$ and the corresponding related function as defined in equation (4) is denoted $G_{\rm as}(\omega)$. Since, in this case, the wave equations are integrated from the surface down to a point in the envelope, by construction $\alpha_{\rm as}$ and $G_{\rm as}$ depend only on the upper layers. The continuous line in Fig. 1 corresponds to $G_{\rm as}(\omega)$ for a solar model without diffusion, (Christensen-Dalsgaard, Proffitt & Thompson 1993), in the following referred to as Model A.

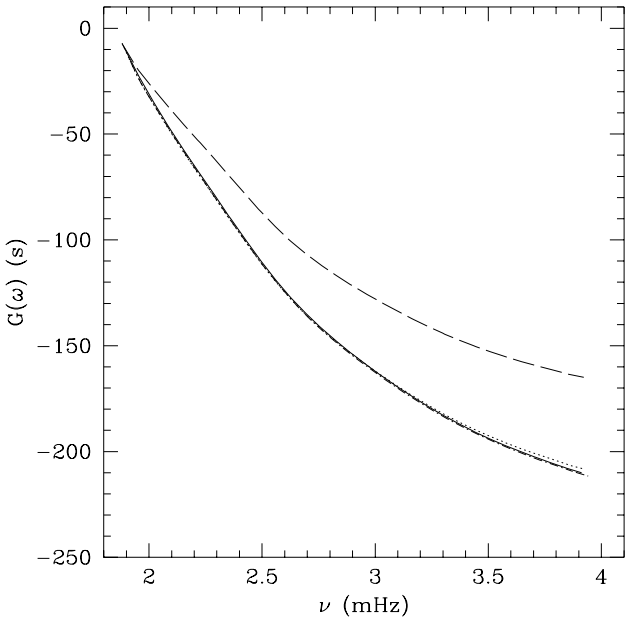

Figure 1. The continuous line is $G_{\rm as}(\omega)$ for Model A. The dashed line is $G(\omega)$ for the same model and the frequency set indicated in the text. The dot-dashed line is $G_{\rm cow}(\omega)$ for the same model and mode-frequency set but in the Cowling approximation. The dotted line is $G + d/\omega^2$, where d is a constant. The functions have been shifted by constants to match at the lowest frequency.

It is interesting to note that the well-known Tassoul equation (Tassoul 1980), which is an approximation valid for low-degree modes,

$$\nu_{nl} \simeq \left(n + \frac{L}{2} + \theta\right)\Delta\nu - \left(AL^2 - \delta\right)\frac{\Delta\nu^2}{\nu_{nl}} \,, \qquad (5)$$

where ν_{nl} is the cyclic frequency and θ, δ, A and $\Delta\nu$ are constants, is a particular case of equation (2). In fact, it is straightforward to show that in this approximation

$$F(w) \simeq \frac{1}{2\Delta\nu} - \frac{\pi}{2w} + \frac{2\pi^2 A\Delta\nu}{w^2} \qquad (6)$$

and

$$G(\omega) \simeq \frac{\pi\theta}{\omega} + \frac{2\pi^2\delta\Delta\nu}{\omega^2} \,. \qquad (7)$$

A detailed derivation of equation (5) from equation (2) was given by Vorontsov (1991) (see also Gough 1986).

If the radial order n and the degree l are assumed to be known, $F(w)$ and $G(\omega)$ can be estimated from p-mode frequencies by fitting them to equation (2). Hence these functions are potentially observable quantities for solar-like stars. This is the advantage of using equation (2) rather than

the formally more precise equation (1). In the present work we have made a least-squares fit, expanding $F(w)$ and $G(\omega)$ in terms of Legendre polynomials in w and ω:

$$\frac{\pi n}{\omega_{nl}} \simeq a_0 + \sum_{i=1}^{k} a_i f_i(x) + \sum_{i=1}^{m} b_i g_i(y) \ , \tag{8}$$

where f_i and g_i are Legendre polynomials of order i with coefficients a_i and b_i. The variables x and y are linearly related to w and ω, respectively, and are defined in the interval $[-1, 1]$. Note that from such a fit $F(w)$ and $G(\omega)$ can be obtained only to within a constant.

Throughout the paper we use the same mode data set, consisting of modes with $l = 0, 1, 2$ and $12 \leq n \leq 27$. The interval in n has been chosen such as to reject modes with very low amplitudes, which are not expected to be observed in solar-like stars. We note that rather similar results are obtained if modes with $l = 3$ are added. The fit was carried out through χ^2 minimization, using frequency errors obtained in early observations with the GOLF instrument on the SoHO spacecraft (Lazrek et al. 1997). In equation (8) we have used Legendre polynomials of order 14 for each function. We note in passing that, as suggested by equation (6), the expansion of $F(w)$ is most reasonably carried out in terms of w^{-1}. In this case a value $k \simeq 5$ in the expansion of $F(w)$ is sufficient to achieve a good fit. But in any case this does not affect to the determination of $G(\omega)$ with which we are mainly concerned in this work.

This kind of fit for $G(\omega)$ is rather similar to that used in inversion techniques (e.g. Dziembowski, Pamyatnykh & Sienkiewicz 1990) though in that case the fit is usually done to a function corresponding to differences between models rather than to $G(\omega)$ directly. On the other hand, Vorontsov, Baturin & Pamyatnykh (1992) applied a very similar fit to solar p modes, but considering modes with higher degrees.

For the Sun, equation (2) is a good approximation for modes of moderate degree, in particular for those modes with inner turning points between the base of the convection zone and the second helium ionization zone. When this kind of mode set is used, the asymptotic function $G_{\rm as}(\omega)$ and the numerically fitted $G(\omega)$ agree very well. Therefore, the observational $G(\omega)$ can be used as a test of the upper layers. However, when only low-degree modes are included, such as is the case for other stars, the approximations leading to equation (2) are not so accurate and hence larger differences between $G_{\rm as}$ and G are expected. This can be seen in Fig. 1, where the dashed line corresponds to $G(\omega)$ for Model A (since G is obtained to within a constant, in Fig. 1 and the following figures we choose the constant such that all the functions agree at a given frequency). Indeed, there are significant differences between $G(\omega)$ and $G_{\rm as}(\omega)$, the main difference coming from neglecting the perturbations in the gravitational potential in equation (2). This can easily be checked by determining the corresponding function $G_{\rm cow}(\omega)$ by fitting to p-mode frequencies computed in the Cowling approximation. This is shown by the dot-dashed line in Fig. 1. It is indeed much closer to $G_{\rm as}$. Thus, the function G obtained from the observations is a sum of $G_{\rm as} \simeq G_{\rm cow}$ that depends on the upper layers and a function that depends on the perturbation in the gravitational potential throughout the solar interior.

For completeness we also note that the function $F(w)$ obtained from a fit to equation (2) does not agree with the asymptotic expression (3), except if the frequencies in the Cowling approximation are used.

2.2 Perturbations on the gravitational potential

In principle, equation (2) can be improved by including the perturbation in the gravitational potential. To first order, the result is an additional term with a specific dependence on ω and L, such that equation (2) is replaced by

$$\frac{\pi n}{\omega_{nl}} \simeq F\left(\frac{\omega}{L}\right) - G(\omega) + \frac{1}{\omega^2} P_\Phi\left(\frac{\omega}{L}\right) \tag{9}$$

(Vorontsov 1991). It is straightforward to show that if $F(w)$, $G(\omega)$ and $P_\Phi(w)$ are solutions of a fit to equation (9) then so are $F(w)+C$, $G(\omega)+C+D/\omega^2$ and $P_\Phi(w)+D$ for any constants C and D. In particular, it is not possible to separate the contributions of the upper layers, as given by $G_{\rm as}$, from the zero-order term of P_Φ since in any fit to observational data both would be included in $G(\omega)$.

We consider again the function G obtained from a fit to equation (2). In Fig. 1 the dotted line represents $G(\omega)+d/\omega^2$ with a suitable (positive) value for the constant d (as well as including the constant shift mentioned above). It is clear that $G \simeq G_{\rm as} - d/\omega^2$. Had we done a fit to equation (9), we would have obtained a similar discrepancy due to the undetermined constant D. Thus, in what concerns the determination of G, a fit to equation (9) is equivalent to a fit to equation (2).

We shall now argue that, when considering a pair of models (or a model and the observations), the differences in P_Φ are very small and hence $\delta G \simeq \delta G_{\rm as}$. To a first approximation, the function P_Φ is given by (e.g. Vorontsov 1991; Christensen-Dalsgaard 1996)

$$P_\Phi\left(\frac{\omega}{L}\right) = 2\pi G \int_{r_{\rm t}}^{R} \rho \left(1 - \frac{L^2 c^2}{\omega^2 r^2}\right)^{-1/2} \frac{{\rm d}r}{c} \ , \tag{10}$$

where ρ is the density. Since we are dealing with low-degree modes, P_Φ can be approximated by a Taylor expansion in $\tilde{w} = L/\omega$ around the centre. From equation (10), we have

$$P_\Phi(\tilde{w} = 0) = 2\pi G \int_0^R \rho \frac{{\rm d}r}{c} \propto \bar{\rho}^{1/2} \int_0^1 \frac{\tilde{\rho}}{\tilde{c}} {\rm d}x \ , \tag{11}$$

where $\bar{\rho}$ is the mean density, $x = r/R$ and $\tilde{\rho}$, $\tilde{c}$ are dimensionless functions. Also, by setting $z = r^2/c^2$ as the independent variable and integrating equation (10) by parts twice, it follows that

$$\left.\frac{{\rm d}P_\Phi}{{\rm d}\tilde{w}}\right|_{\tilde{w}=0} = 0 \ . \tag{12}$$

Thus, the variation of P_Φ is of second order in $\tilde{w}$, and in the $\tilde{w}$ interval spanned by our data set P_Φ can be estimated by its value at the centre.

From equation (11), it follows that, for models with the same mean density and similar structure in the inner region, the functions P_Φ are similar; hence, when considering differences between pair of such models, this term can be neglected. In fact, numerical tests show that for realistic solar models the differences between $G(\omega)$ are very close to the corresponding differences in $G_{\rm as}(\omega)$. Hence, although

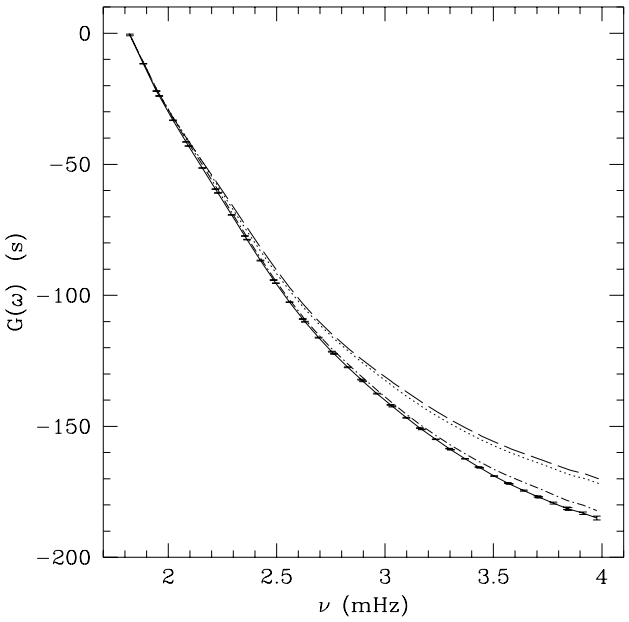

Figure 2. The function $G(\omega)$ for the observations (continuous line with error bars), Model A (dashed line), Model B (dotted line) and Model C (dot-dashed line). The functions have been shifted by constants to match at the lowest frequency.

the function $G(\omega)$ depends also on properties of the interior, differences between such functions depend mainly on the differences between the uppermost layers. For distant stars the mean density is generally not known with sufficient accuracy; however, in this case it is likely that similar cancellation can be achieved by working in terms of frequencies measured in units of the large frequency separation $\Delta\nu_{nl} = \nu_{nl} - \nu_{n-1\,l}$ (cf. equation 5) which scales approximately as $\bar{\rho}^{-1/2}$.

In order to illustrate the dependence of $G(\omega)$ on stellar structure, in Fig. 2 we show this function for three solar models and the mode set indicated above. The dashed line corresponds to the previously mentioned Model A, the dotted line to a model that includes helium settling (Christensen-Dalsgaard, Proffitt & Thompson 1993, hereafter Model B) and the dot-dashed line to a solar model that in addition has an artificial increase in the surface opacities in order to get a better agreement with the observations (hereafter Model C). As a result of helium settling, the envelope helium abundance $Y_{\rm env} \simeq 0.25$ of Models B and C is lower than the value $\simeq 0.28$ for Model A. On the other hand, Model C differs substantially from the other two in the uppermost layers. As can be seen, the function $G(\omega)$ for this model is also significantly different. In Fig. 2 we also show $G(\omega)$ computed with the observed frequencies (Lazrek et al. 1997), with errors estimated by Monte-Carlo simulation. As expected, Model C is closest to the observational data. (Note that, since the superficial layers of the solar model suffers from other uncertainties, such as non-adiabatic and convective effects, it cannot on this basis be concluded that Model C is better than the other two.) This result is similar to that obtained by using intermediate-degree modes.

For distant stars with poorly known parameters, the uncertainty in $P_\Phi(0)/\omega^2$ can eventually become comparable with the differences in $G_{\rm as}$. In this case, it may be better to work with a phase function invariant under the transformation $G' \rightarrow G+C+D/\omega^2$ or, equivalently, $\alpha' \rightarrow \alpha+C\omega+D/\omega$. It is easy to show that the phase function

$$\gamma = \alpha - \omega\frac{{\rm d}\alpha}{{\rm d}\omega} - \omega^2\frac{{\rm d}^2\alpha}{{\rm d}\omega^2} \tag{13}$$

has this property and hence depends only on the upper layers. This is a generalization of

$$\beta = \alpha - \omega\frac{{\rm d}\alpha}{{\rm d}\omega}\ , \tag{14}$$

which has been used in earlier investigations (e.g. Brodsky & Vorontsov 1988; Christensen-Dalsgaard & Pérez-Hernández 1991; Lopes et al. 1997), and which is invariant only under the transformation $\alpha' \rightarrow \alpha + C\omega$.

We note that the function γ introduces a filter which suppresses partially the contribution of the uppermost layers. Thus, if a good estimate of the uncertainty in P_Φ as given by equation (11) is available, it is generally better to work with $\alpha(\omega)$ or $G(\omega)$. On the other hand, if we are interested in deeper layers (such as the second helium ionization zone), then the filtering procedure described below may be preferable, in isolating more effectively the contribution from just these layers.

2.3 The filtered phase function

Although G depends mainly on the uppermost layers, it also has a small contribution from deeper layers. In fact, it is possible to obtain from $G(\omega)$ a function which predominantly reflects the properties of the layers around the second helium ionization zone.

Pérez Hernández & Christensen-Dalsgaard (1994a) showed how a similar function can be extracted through a filter. Rather than equation (2), they considered an equivalent expression for differences, assumed to be small, between pairs of models. With this assumption the differences between phase functions are linearly related to differences between the equilibrium models (Christensen-Dalsgaard & Pérez Hernández 1992) by

$$\mathcal{H}_2 \equiv \frac{\pi\delta\alpha}{\omega} \simeq \int_{r_0}^{R}\left[K_c(r)\frac{\delta c}{c}(r) + K_{\omega_{\rm a}}(r)\frac{\delta\omega_{\rm a}}{\omega_{\rm a}}(r)\right]{\rm d}r\ , \tag{15}$$

where $\omega_{\rm a}$ is the Lamb acoustical cut-off frequency and the kernels K_c and $K_{\omega_{\rm a}}$ are known functions. Due to the behaviour of the kernels in the solar interior, a localized perturbation has a frequency dependence of the form (Pérez Hernández & Christensen-Dalsgaard, 1994a)

$$\mathcal{H}_2 \propto \cos 2\big[\omega\tau - (\alpha+1/4)\pi\big]\ , \tag{16}$$

where τ is the acoustical depth,

$$\tau = \int_r^R \frac{1}{c}{\rm d}r\ . \tag{17}$$

Hence shorter-period components in $\mathcal{H}_2$ correspond to perturbations in deeper layers. Thus by filtering the smooth components of $\mathcal{H}_2$ it is possible to obtain a function $\mathcal{H}_2^{\rm f}$ that depends on deeper layers.

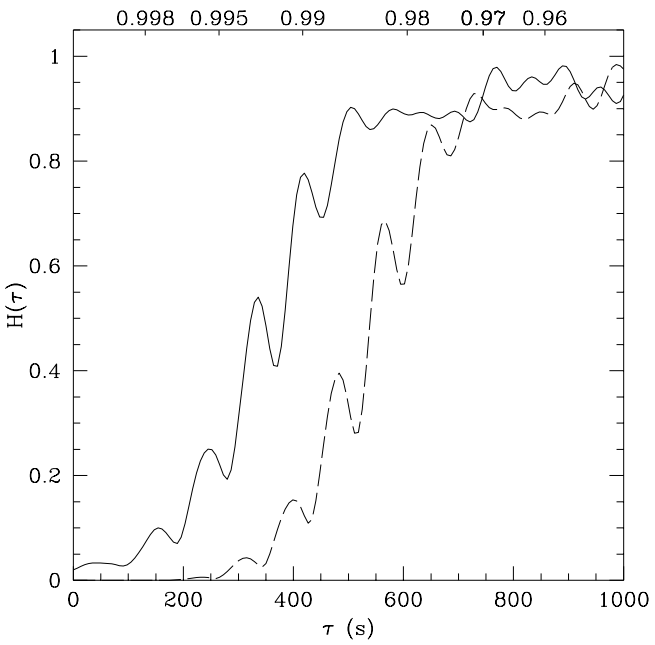

Figure 3. Response function $H(\tau)$ as function of acoustical depth τ and radius (on top). The solid line is for equation (20) and the dashed line for harmonic functions, both for fits with $p = 6$.

In the present case, $G(\omega)$ can be thought of as the difference between the actual model (or the Sun) and a smoothed model that does not have this localized feature. Relation (16) is then still valid and we can obtain a filtered $G^{\rm f}$ in a similar way to $\mathcal{H}_2^{\rm f}$.

The filter used by Pérez Hernández & Christensen-Dalsgaard (1994a) was a recursive filter especially suitable for $\mathcal{H}_2$ because of the flatness of its smooth component at low frequencies ($\nu \leq 1.4$ mHz for the Sun). In the stellar case modes at such low frequencies are unlikely to be observed because of their expected low surface amplitudes. Furthermore, for the function G, upon which much of our analysis is based, the smooth component does not have this behaviour. However, below we describe a different filter which has similar properties and can be extracted directly from the least-squares fit used to compute $G(\omega)$.

Since, in the present work, we obtain G as a Legendre polynomial expansion, a simple way of separating the smooth and oscillatory frequency patterns is to consider the low- and high-order polynomial coefficients, respectively. A very similar type of filtering was introduced by Vorontsov et al. (1992). Specifically, we define

$$G^{\rm f}(\omega) = \sum_{i=p+1}^{m} b_i g_i(\omega) \; . \tag{18}$$

A suitable value of p will give the desired oscillatory function. Similarly, the asymptotic function $G_{\rm as}$ can be fitted to Legendre polynomials, from which $G_{\rm as}^{\rm f}$ may be defined.

In order to choose the value of p in equation (18), we have computed the response to the filtering of signals of the form (16). Specifically, we define the response function $H(\tau)$ by

$$H(\tau) = \frac{\sum_i y_i^2(\omega_i, \tau)}{\sum_i x_i^2(\omega_i, \tau)} \; , \tag{19}$$

where $x(\omega, \tau)$ is the input signal and $y(\omega, \tau)$ is the output function, calculated as in equation (18) by expanding $x(\omega, \tau)$ in Legendre polynomials of order m and setting to zero the first p terms; the summation is over the frequency range considered. Here we have used the observed frequencies of Lazrek et al. (1997).

We consider filtering corresponding to $p = 6$. The dashed line in Fig. 3 shows the response to simple harmonic functions $x_i = \cos(2\omega_i \tau)$. However, since in equation (16) α is a function of frequency, the contribution to $G(\omega)$ of a given layer is not exactly a harmonic function. To investigate the effect of this, in equation (19) we take as input

$$x_i = \cos 2\big[\omega_i \tau - (\alpha_{\rm as}(\omega_i) + 1/4)\pi\big] \; , \tag{20}$$

with $\alpha_{\rm as}$ computed for a given solar model. The solid line in Fig. 3 corresponds to $H(\tau)$ calculated in this way, with $\alpha_{\rm as}$ obtained from Model A. This term clearly has a significant effect, corresponding approximately to a shift in τ. From the figure, it follows that the filter considered suppresses most of the signal from the uppermost layers ($r > 0.997R$) while passing the signal from $r \sim 0.98R$, where the second helium ionization zone is located. Hence in the following we shall take $p = 6$ in equation (18), at least for the Sun.

In Fig. 4 we show $G_{\rm as}^{\rm f}(\omega)$ and $G^{\rm f}(\omega)$ for a solar model. The dashed line corresponds to $G_{\rm as}^{\rm f}$, the dot-dashed line to $G_{\rm cow}^{\rm f}$ computed in the Cowling approximation and the solid line to $G^{\rm f}$ using the full equations. Since $G^{\rm f} \simeq G_{\rm cow}^{\rm f}$, $G^{\rm f}$ does not depend on the perturbations in the gravitational potential. Furthermore, since $G^{\rm f} \simeq G_{\rm as}^{\rm f}$, the function $G^{\rm f}$ depends on the layers between r_0 (a point in the adiabatically stratified convection zone) and an upper limit given by the response function, as in Fig. 3.

In Fig. 5 we show $G^{\rm f}(\omega)$ for the same solar models as in Fig. 2. The function $G^{\rm f}$ is very similar for Models B and C, showing that the filtering has suppressed the substantial difference in G between Models B and C (cf. Fig. 2), caused by the differences in the structure of the superficial layers. On the other hand $G^{\rm f}$ for Model A is clearly different, reflecting the differences in the equilibrium structure in the second helium ionization zone. As shown by Pérez Hernández and Christensen-Dalsgaard (1994b) this kind of filtered phase function depends on three main properties: the equation of state, the helium abundance $Y_{\rm env}$ in the envelope and the specific entropy s in the adiabatically stratified part of the convection zone, whose value controls the depth of the convection zone. Model A has the same equation of state than Models B and C but $Y_{\rm env}$ is larger and the depth of the convection zone smaller. In Fig. 5 we also show $G^{\rm f}$ for the observations (Lazrek et al. 1997), with errors determined from a Monte-Carlo simulation. It can be seen that the models with diffusion (and hence $Y_{\rm env} \simeq 0.25$ and a depth of the convection zone closer to that inferred from sound speed inversions) agree better with the observations. This is in accordance with the the analysis with moderate-degree modes, as shown in Pérez Hernández & Christensen-Dalsgaard (1994b). Although in the present case the errors are larger, our purpose is to show that by using low-degree modes alone it is possible to carry out a similar analysis for the distant stars.

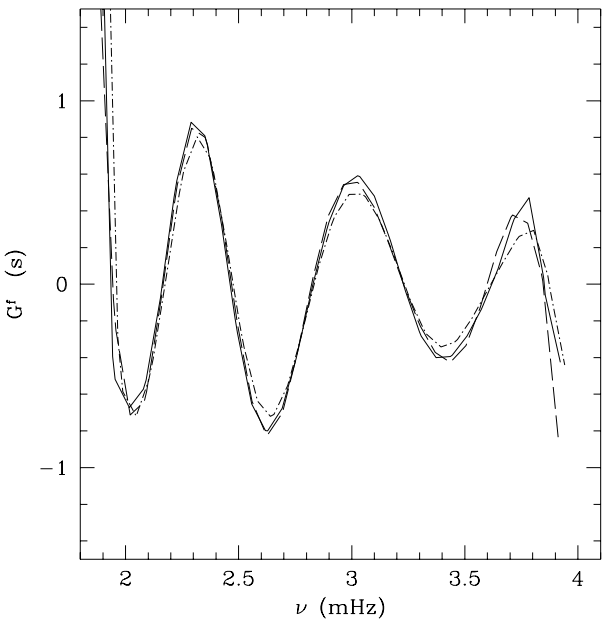

Figure 4. The dashed line is $G^{\rm f}_{\rm as}(\omega)$ for Model A. The solid line is $G^{\rm f}(\omega)$ for the same model and the dot-dashed line the same function but using p-mode frequencies in the Cowling approximation.

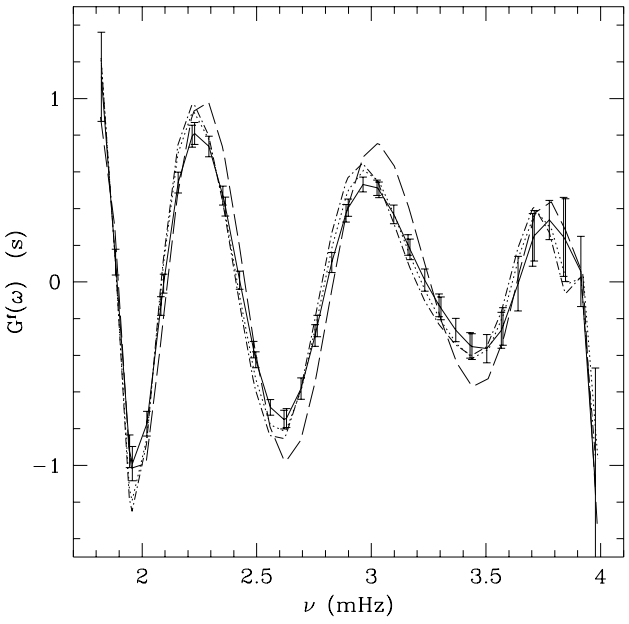

Figure 5. The continuous line with error bars is $G^{\rm f}$ for the observations, the dashed line is $G^{\rm f}$ for Model A, the dotted line is for Model B, and the dot-dashed line is for Model C.

3 PHASE FUNCTION FOR STARS

3.1 Global properties

In this section we shall consider the phase functions $G(\omega)$ and $G^{\rm f}(\omega)$ for models of stars on the main sequence. The models considered are summarized in Table 1. There are two models for each mass, one at the zero-age main sequence and the other near the end of hydrogen burning. We shall consider the same mode set than for the Sun, that is $l = 0, 1$ and 2 and $12 \leq n \leq 27$. To obtain estimates of the errors in these functions we assume normally distributed frequency errors with $\sigma = 0.5$ μHz.

Table 1. Stellar models considered. X_c is the central hydrogen abundance

model	$M/M_\odot$	$X_{\rm c}$	$L/L_\odot$	$T_{\rm eff}$
1	0.85	0.6928	0.329	5038
2	0.85	0.0003	0.891	5466
3	1.00	0.6928	0.718	5628
4	1.00	0.1004	1.238	5813
5	1.30	0.6928	2.572	6509
6	1.30	0.0516	3.695	6142
7	1.70	0.6928	8.512	8071
8	1.70	0.0479	10.994	6619

Fig. 6 show $G_{\rm as}$ – dashed line – and $G(\omega)$ with the corresponding errors – continuous line – for all the models considered. As for the solar case, most of the differences between $G_{\rm as}$ and G can be represented as a function of the form d/ω^2, as shown in the figures (the dot-dashed lines correspond to $G + d/\omega^2$). We have also computed $G(\omega)$ in the Cowling approximation. Although for clarity we do not show it here, we note that in most of the cases $G_{\rm as} \simeq G_{\rm cow}$, and hence the same comments apply as for the Sun.

However, for the models at the end of hydrogen burning, and in particular for the most massive ones, the agreement between $G_{\rm as}$ and $G_{\rm cow}$ is worse, hence indicating that other simplifications leading to equation (2) are not so good for these models. In fact, as the stars evolve, the buoyancy frequency increases in the core. This effect is more significant for models with shrinking convective cores, that is, for relatively massive stars. As a result, the term in N^2 in equation (1) must be taken into account, and hence the simple asymptotic expression in equation (2) is no longer adequate. Furthermore, the buoyancy frequency introduces additional effects in the correction for the perturbation to the gravitational potential. [For more complete discussions, see for example Vorontsov (1991); Gough (1993); Roxburgh & Vorontsov (1994).] Indeed, as shown in Fig. 6, the differences between G and $G_{\rm as}$ for the evolved models are not exactly of the form d/ω^2. Thus analysis of data with very small errors requires an asymptotic description which is more accurate than equation (2).

To compute the filtered function $G^{\rm f}$ we first look for the value of p in equation (18). The goal of the analysis is to isolate the signature of the second helium ionization, as was done in the solar case in Fig. 5. Thus the optimal value of p must reflect the acoustical depth of the ionization region, as indicated by equation (16). The location of the second helium ionization varies in temperature from about 1.2×10^5 K in Model 1 to 4.7×10^4 K in Model 7; this variation, combined with the change in the stellar surface temperature, changes the acoustical depth of the associated variation in Γ_1. This is illustrated in Fig. 7 for a selection of the models in Table 1; here Γ_1 is plotted against the relative acousti-

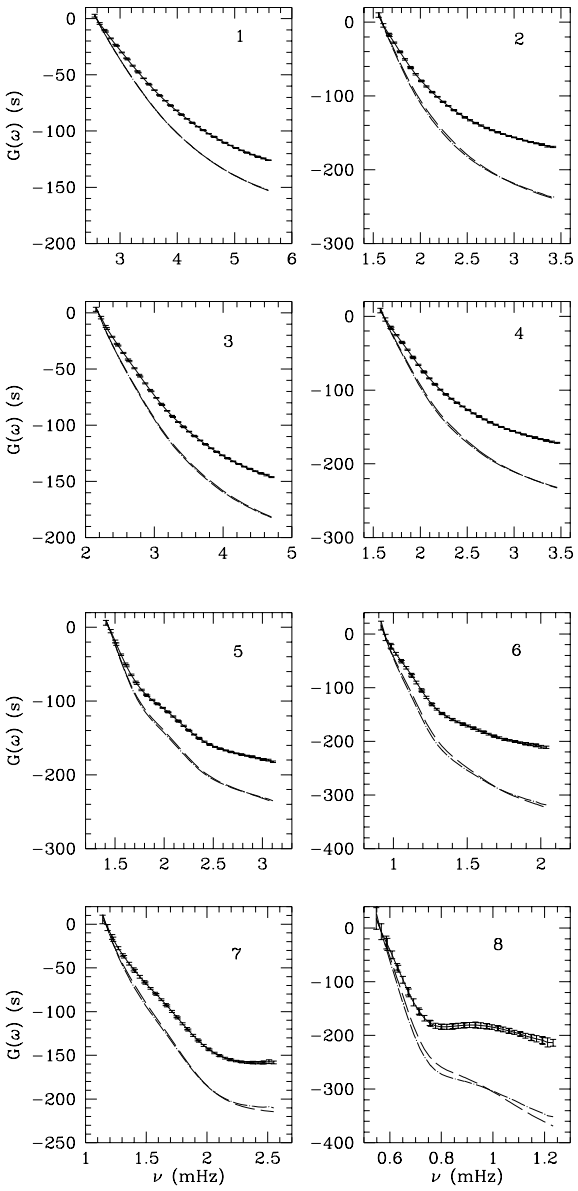

Figure 6. The dashed line is $G_{\rm as}$, the continuous line with error bars is G and the dot-dashed line $G + d/\omega^2$ for the model of Table 1 indicated in each panel. To all the functions we have added a constant so that they match at the lowest frequency.

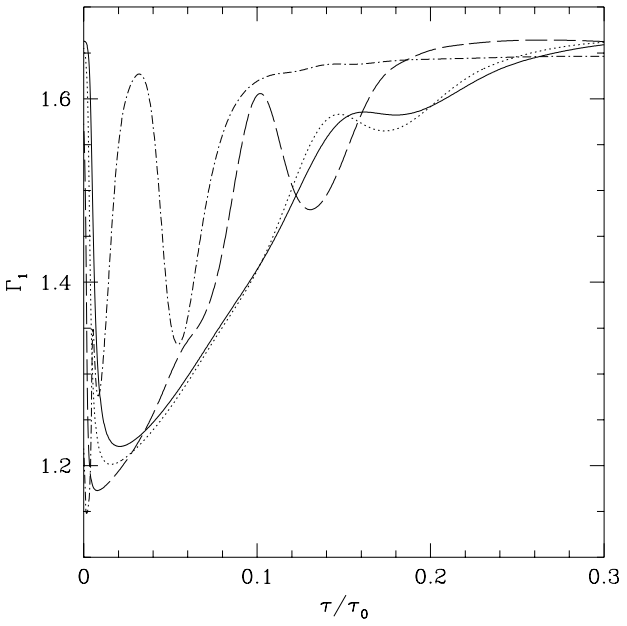

Figure 7. Γ_1 as function of relative acoustical depth τ/τ_0 for the ZAMS models in Table 1. The continuous line is for Model 1, the dotted line for Model 3, the dashed line for Model 5 and the dot-dashed line for Model 7.

cal depth τ/τ_0, where τ_0 is the acoustical radius of the star, obtained by integrating from $r = 0$ in equation (17).

To determine the optimal p, we calculate the response function $H(\tau)$ given by equation (19) for different values of p. Here the frequency interval and $\alpha_{\rm as}$ are computed for each model in Table 1. Then we choose p so as to keep the information from the second helium ionization zone, here defined at the point where Γ_1 has a relative minimum. We have found that for Models 1 to 6 in Table 1 a value of $p = 6$ is suitable. For Model 7 a value of $p = 2$ has been chosen, and for Model 8, $p = 3$. This decrease of p with increasing effective temperature clearly reflects the fact that the second helium ionization zone moves closer to the surface.

Fig. 8 shows the functions $G^{\rm f}(\omega)$ for the stellar models. We note that for all the models considered the filtered function $G^{\rm f}$ agrees within the errors with the asymptotic $G^{\rm f}_{\rm as}$ (which, for clarity, we do not show). As can be seen, for the models with $M = 0.85\ M_\odot$, it is not possible to detect the signature of the HeII zone as given by $G^{\rm f}$ even with frequency errors as small as $0.5\,\mu$Hz. However, for the rest of the models this frequency accuracy is sufficient. Also, from the figure it follows that $G^{\rm f}(\omega)$ has a larger amplitude for larger masses or later evolution stages, due to the increased strength of the He-II feature in Γ_1 (cf. Fig. 7; see also Lopes et al. 1997). It can also be seen that in the fixed range of radial orders considered, $G^{\rm f}$ contains fewer periods of the signal for $M = 1.7\ M_\odot$ than for the other masses. Indeed, it follows from equation (5), with $\Delta\nu \simeq (2\tau_0)^{-1}$, that in equation (16) $2\omega\tau \simeq 2\pi n\tau/\tau_0$. Thus for a fixed range in n, such as we have considered here, the signal arising from the second helium ionization zone generally oscillates less rapidly with decreasing relative depth τ/τ_0.

3.2 Changes to the physics and parameters of the models

We have considered several changes to the input physics and stellar parameters in order to analyse the sensitivity of the phase function to such quantities. Since, once the p-mode frequencies of a star are measured, the mean density can be accurately determined, it is interesting to compare models with the same mean density, considering the effects of each modification separately. To do so, we have computed envelope models which have boundary conditions only at the surface, considering models with the same surface parameters as those given in Table 1. For each of these eight models we have considered the modifications summarized

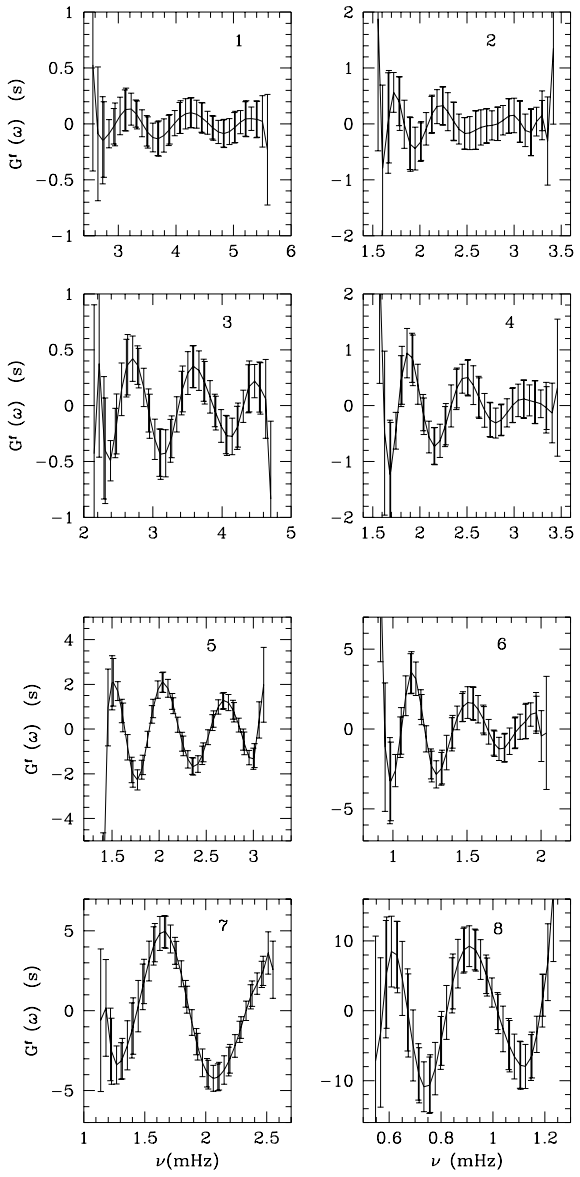

Figure 8. $G^{\rm f}(\omega)$ for the model in Table 1 indicated in each panel.

in Table 2. Here $\alpha_{\rm c}$ is the mixing length parameter, X the hydrogen abundance, κ the opacity, r_c the radius at the base of the convection zone and EOS refers to the equation of state; all the models use the EFF formulation (Eggleton, Faulkner & Flannery 1973), except for the model corresponding to change 6 which uses the CEFF equation of state (see Christensen-Dalsgaard & Däppen 1992). For envelope models it is not possible to compute low-degree p-mode frequencies, and hence we cannot obtain $G(\omega)$ from a fit to equation (2). However, as remarked previously, the differences in the function G for the models corresponding to the small modifications considered in Table 2 can be expected to be very similar to those in $G_{\rm as}$, which can be computed for envelope models.

As an illustrative case, we shall show the results for just one case, an envelope model with the same global and surface parameters as Model 5 in Table 1. In Fig. 9 we show

Table 2. Modifications to the envelope models.

	parameter	magnitude	notes
1	$T_{\rm eff}$	+100 K	
2	$\alpha_{\rm c}$	-0.2	
3	X	-0.01	at constant Z
4	$\log_{10}\kappa$	-0.2 in atmosphere	at fixed r_c
5	Z	+0.005	at constant X
6	EOS	CEFF	

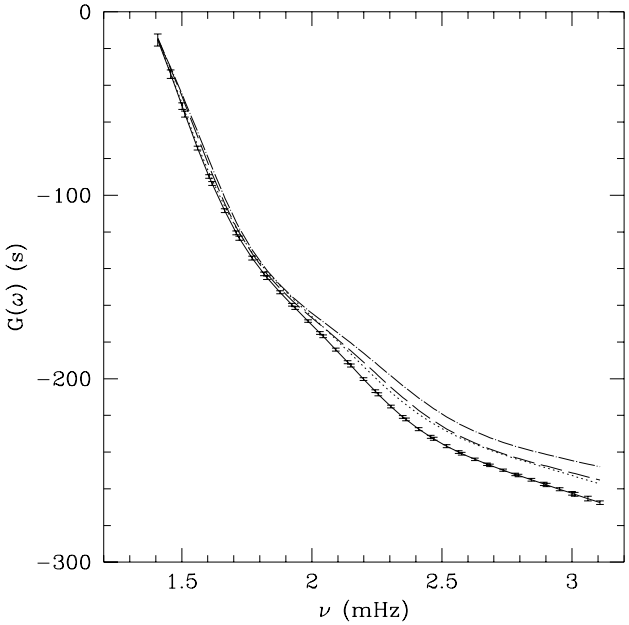

Figure 9. The continuous line is $G_{\rm as}(\omega)$ for an envelope model similar to Model 5 in Table 1. The dashed line corresponds to the change in $T_{\rm eff}$, the dot-dashed line to the change in the mixing-length parameter $\alpha_{\rm c}$, and the dotted line to the change in the atmospheric opacity, for the changes listed in Table 2. The functions have been shifted by constants to match at a given frequency.

$G_{\rm as}(\omega)$ for several modifications. The continuous line is for the reference model with errors corresponding to frequency errors of 0.5 μHz. The dashed line corresponds to the change in $T_{\rm eff}$, the dot-dashed line to the change in the mixing-length parameter $\alpha_{\rm c}$, and the dotted line to the change in the atmospheric opacity. The functions $G_{\rm as}$ for the changes in X, Z and the equation of state are not shown because they differ from $G_{\rm as}$ for the reference model by less than the errors. This could be expected since these modifications do not change significantly the structure of the uppermost layers, contrary to those shown in the figure. Similar results are found for the other models in Table 1.

From Fig. 9, it follows that the function G computed from the observations can be used to constrain the structure of the uppermost layers. However, it is also clear that it is not possible to isolate one uncertainty from the rest, at least with an analysis of a single star.

In Fig. 10, we show the differences $\delta G^{\rm f}_{\rm as}(\omega)$ between the models with the changes indicated in Table 2 and the refer-

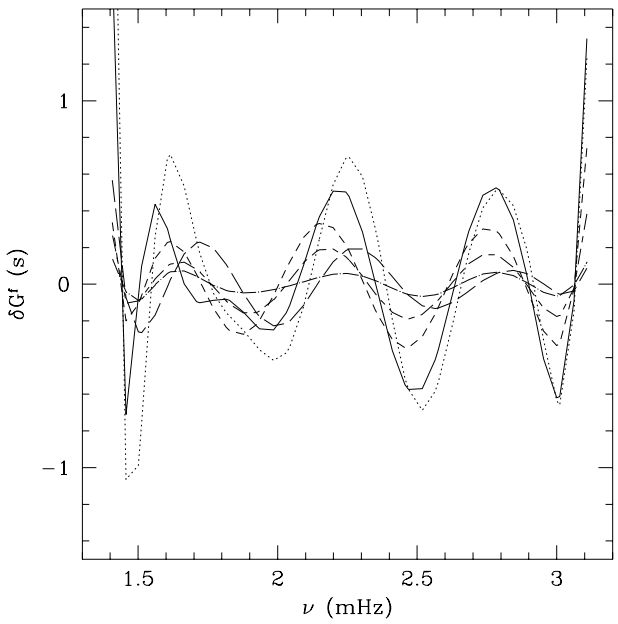

Figure 10. Differences in the filtered phase-function $G^{\rm f}_{\rm as}$ between envelope models with the modifications indicated in Table 2 and the reference model (corresponding to Model 5 in Table 1) for: change in $T_{\rm eff}$ (continuous line), change in the mixing length parameter $\alpha_{\rm c}$ (dotted line), change in the atmospheric opacities (long dashed line), change in X (dot-dashed line), change in Z (short-long dashed line) and change in the equation of state (short dashed line).

ence model (an envelope model corresponding to Model 5 in Table 1). As expected, $\delta G^{\rm f}$ is significant for the change in the equation of state or the envelope abundances, as a result of the corresponding changes in Γ_1 in the second helium ionization zone; however, it is also important for modifications in the atmospheric opacities or the mixing-length parameter $\alpha_{\rm c}$ because these modifications change, for instance, the depth of the second helium ionization layer. This result is roughly similar to that found for the Sun (see Pérez Hernández & Christensen-Dalsgaard 1994b), although the relative importance of each modification is different.

For clarity we have not shown the errors in Fig. 10 but we note here that for frequency errors of $0.5\,\mu$Hz, the mean error in $G^{\rm f}$ is of 0.42 s and for $0.1\,\mu$Hz, the mean error in $G^{\rm f}$ is 0.08 s. Hence, very accurate frequency determinations are required in order to obtain information from this function, in particular concerning the envelope abundances or the equation of state.

4 CONCLUSIONS

By analysing low-degree ($l \leq 2$) p-mode frequencies for the Sun we have shown that it is possible to fit an asymptotic expression which allows to separate the contribution of the upper layers as given by a function of frequency $G(\omega)$ from that of the interior. Moreover, it is possible to obtain a function $G^{\rm f}(\omega)$ that depends mainly on the layers around the second helium ionization zone. By applying the same technique to p-mode frequencies of stellar models, we have found that the same separation is possible for main-sequence stars with masses between 0.85 $M_\odot$ and 1.7 $M_\odot$.

Of course, the main goal is to get information about stellar structure from these functions. When considering observed solar frequencies of low-degree modes, we have found that the function $G(\omega)$ is determined with sufficient accuracy to impose constraints on the structure of the uppermost layers of the Sun. Assuming frequency errors of $0.5\,\mu$Hz we found that the same can be true for other stars. Although different changes to the physics and parameters of the models can lead to very similar $G(\omega)$, it might be possible to separate the effects of different uncertainties if several stars, belonging to the same cluster, are analysed; in this case it may be assumed, for example, that the stars share the same initial composition.

In principle, analysis of the function $G^{\rm f}$ could provide more significant constraints on the stellar models because it depends on the structure of the layers around the second helium ionization zone, where the physics is better understood than in the uppermost layers. However, very small errors are needed in order to obtain useful information from it. For instance, in the solar case, if only low-degree modes are used, frequency errors as small as those achieved by GOLF are required in order to determine the helium abundance in the solar envelope. Similar results are found for stars in the main sequence, for which errors substantially below $0.5\,\mu$Hz are needed in order to impose significant constraints on the stellar models, for instance for the helium abundance or the equation of state. It is encouraging, therefore, that the COROT mission (Catala et al. 1995) aims at determining frequencies with errors as small as $0.1\,\mu$Hz. We note also that $G^{\rm f}$ is more sensitive to modifications in the equilibrium structure for stars of mass greater than solar.

ACKNOWLEDGEMENTS

This work has been made possible thanks to the financial support from the Spanish DGICYT under grants ESP90-0969 and PB91-0530, and from the Danish National Science Foundation through its establishment of the Theoretical Astrophysics Center.

REFERENCES

Baglin A., 1991, Solar Phys. 133, 155

Brown T. M., Gilliland R. L., Noyes R. W., Ramsey L. W., 1991, ApJ 368, 599

Brodsky M. A., Vorontsov S.V., 1988, in Christensen-Dalsgaard J., Frandsen S., eds, Proc. IAU Symp. 123, Advances in Helio- and Asteroseismology. Reidel, Dordrecht, p. 137

Catala C., Auvergne M., Baglin A. et al. 1995, in Hoeksema J. T., Domingo V., Fleck V., Battrick B., eds, ESA Symp. 376, Proc. 4th SOHO Workshop: Helioseismology, Vol. 2. ESTEC, Noordwijk, p. 549

Christensen-Dalsgaard J., 1984, in Praderie F., ed., Space Research Prospects in Stellar Activity and Variability. Paris Observatory Press, p. 11

Christensen-Dalsgaard J., 1988, in Christensen-Dalsgaard J., Frandsen S., eds, Proc. IAU Symp. 123, Advances in helio- and asteroseismology. Reidel, Dordrecht, p. 295

Christensen-Dalsgaard J., 1993, in Brown T. M., ed., ASP Conf. Ser. 42, Proc. GONG 1992: Seismic investigation of the Sun and stars. ASP, San Francisco, p. 347
Christensen-Dalsgaard, 1996, in Roca Cortés T., Sánchez F., eds, The Structure of the Sun. Cambridge University Press, p. 47
Christensen-Dalsgaard J., Däppen W., 1992, A&AR 4, 267
Christensen-Dalsgaard J., Pérez Hernández F., 1991, in Gough D. O. & Toomre J., eds, Lecture Notes in Physics. Springer, Heidelberg, 388, 43
Christensen-Dalsgaard J., Pérez Hernández F., 1992, MNRAS 257, 62
Christensen-Dalsgaard J., Gough D. O., Thompson M. J., 1989, MNRAS 238, 481
Christensen-Dalsgaard J., Proffitt C.R., Thompson M., 1993, ApJ. 403, L75
Deubner F.-L., Gough D. O., 1984, ARA&A 22, 593
Dziembowski W., Pamyatnykh A. A., Sienkiewicz R., 1990, MNRAS 244, 542
Eggleton P. P., Faulkner J., Flannery B. P., 1973, A&A 23, 325
Gough D. O., 1986, in Osaki Y., ed., Hydrodynamic and magnetohydrodynamic problems in the Sun and stars, Department of Astronomy, University of Tokyo, p. 117
Gough D. O., 1987, Nature 326, 257
Gough D. O., 1993, in Zahn J.-P., Zinn-Justin J., eds , Astrophysical fluid dynamics, Les Houches Session XLVII. Elsevier, Amsterdam, p. 399
Gough D.O., 1996, in Roca Cortés T., Sánchez F., eds, The Structure of the Sun. Cambridge University Press, p. 141
Gough D. O., Novotny E., 1993, in Brown T. M., ed., ASP Conf. Ser. Vol. 42, Proc. GONG 1992: Seismic investigation of the Sun and stars. Astron. Soc. Pac., San Francisco, p. 355
Kjeldsen H., Bedding T. R., Viskum M., Frandsen S., 1995, AJ 109, 1313
Lazrek M., Baudin F., Bertello L., Boumier P., Charra J., Fierry-Fraillon D., Fossat E., Gabriel A. H., García R. A., Gelly B., Gouiffes C., Grec G., Pallé P. L., Pérez Hernández F., Régulo C., Renaud C., Robillot J.-M., Roca-Cortés T., Turck-Chièze S., Ulrich R. K., 1997, Solar Phys., submitted
Lopes I., Turck-Chièze S., Michel E., Goupil M.-J., 1997, ApJ 480, 794
Pérez Hernández F., Christensen-Dalsgaard J., 1994a, MNRAS 267, 111
Pérez Hernández F., Christensen-Dalsgaard J., 1994b, MNRAS 269, 475
Pottasch E. M., Butcher H. R., van Hoesel F. H. J., 1992, A&A 264, 138
Roxburgh I. W., Vorontsov S. V., 1994, MNRAS 268, 143
Tassoul, M., 1980, ApJS 43, 469
Ulrich R. K., 1986, ApJ 306, L37
Vorontsov S. V., 1991, Astron. Zh. 68, 808 (English translation: Sov. Astron. 35, 400)
Vorontsov S. V., Baturin V. A., Pamyatnykh A. A., 1992, MNRAS 257, 32